

# Electrodeposition of Sn–Co alloys from gluconate baths

S. S. ABD EL REHIM, S. A. REFAEY

*Chemistry Department Faculty of Science, Ain Shams University, Cairo, Egypt*

G. SCHWITZGEBEL

*Physikalische Chemie, FB 11.3, BAU 9, Universität des Saarlandes 66041 Saarbrücken, Germany*

F. TAHA, M. B. SALEH

*Chemistry Department, Faculty of Science, Minia University, Minia, Egypt*

Received 1 June 1995; revised 29 August 1995

Electrodeposition of Sn–Co alloys was carried out from baths containing 2–20 g dm<sup>-3</sup> SnSO<sub>4</sub>, 4–18 g dm<sup>-3</sup> CoSO<sub>4</sub>.7H<sub>2</sub>O, C<sub>6</sub>H<sub>11</sub>O<sub>7</sub>Na and K<sub>2</sub>SO<sub>4</sub> under different conditions of bath composition, pH, current density and temperature on to copper substrates. The influence of these variables on the cathodic potential, cathodic current efficiency and composition of the deposit were studied. The results show that the deposition of Sn–Co alloys from gluconate baths depends greatly on the concentration of tin. At high tin concentrations, tin is the more noble component. At low tin concentrations, tin reduction is strongly suppressed due to the formation of a more stable Sn-gluconate complex species and tin becomes the less noble component. The codeposition of Sn–Co alloy from these baths can be classified as an irregular plating system. The surface morphology of deposits was examined by scanning electron microscopy and crystal structure by X-ray. The results show that the structure of the deposits was controlled by the alloy composition.

## 1. Introduction

Tin–cobalt plating has found extensive application as a convenient and economic way of providing an attractive finish for fasteners, office equipment, hinges, kitchen utensils, hand tools, tubular furniture and motor car interior trim and fittings [1]. Jennison and Bradley [2] described the electrodeposition of tin–cobalt from alkaline media. Ireland and Parkinson [3] electroplated tin–cobalt alloys from fluoride bath. Sree and Rama Char [4] investigated the electrodeposition of this alloy from pyrophosphate bath, the results showed that at low current density (0.7 A dm<sup>-2</sup>) the deposits contained only a few percent of cobalt (the less noble metal) but at high current densities (7.0–8.9 A dm<sup>-2</sup>) the percent of cobalt in the deposit increased and approached the metal percentage of the cobalt in the bath. Clark *et al.* [5] obtained white alloys from a mixed chloride/fluoride bath. Hemsley and Roper [1] electroplated bright tin–cobalt alloys from a bath containing stannous and cobalt sulphates, sodium gluconate as a chelating agent and sodium sulphate as supporting electrolyte. The authors studied the effect of some operating variables on the physical and mechanical properties of the deposits. The appearance of the deposits are similar to chromium and they are sufficiently hard and wear resistant to allow use in most decorative and domestic applications.

Therefore, it was felt that it would be interesting to

study systematically the electrodeposition of tin–cobalt alloys from gluconate baths. The present study deals with the effects of some plating variables on cathodic polarization, cathodic current efficiency and composition and structure of the deposits.

## 2. Experimental details

Experiments were carried out in solutions containing SnSO<sub>4</sub>, CoSO<sub>4</sub>.7H<sub>2</sub>O, C<sub>6</sub>H<sub>11</sub>O<sub>7</sub>Na and K<sub>2</sub>SO<sub>4</sub>. All solutions used were freshly prepared with doubly distilled water and analytical grade chemicals. The pH was adjusted using sulphuric acid or sodium hydroxide. The experimental setup used was described previously [6] and consisted of a rectangular Perspex cell equipped with a plane copper cathode and a platinum sheet anode. Each electrode had dimension 2.5 × 3 cm and filled the cross-section of the cell. Before each run, the cathode was mechanically polished with 600 mesh emery paper, washed with distilled water, rinsed with ethanol and weighed. The experiments were conducted at the required temperatures with the help of an air thermostat. The plating duration was 30 min, after which the cathode was withdrawn, washed with distilled water, dried and weighed. The composition of the deposits was determined by EDX-ray spectrometer (Cam Scan Cambridge Scanning Company Ltd) X-ray diffraction analysis was carried out by X-ray diffractometer (Siemens D 500/501). The morphology of the deposits was examined by scanning

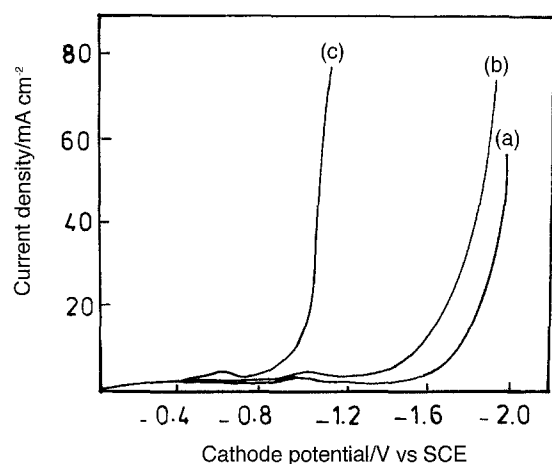


Fig. 1. Cathodic polarization curves for the tin deposition at 25°C from solutions containing 20 g dm<sup>-3</sup> K<sub>2</sub>SO<sub>4</sub> and 32 g dm<sup>-3</sup> sodium gluconate and different concentrations of SnSO<sub>4</sub>: (a) 2, (b) 5, and (c) 20 g dm<sup>-3</sup>.

electron microscopy (Cam Scan Cambridge Scanning Company Ltd).

Potentiodynamic cathodic polarization curves were traced by the use of a potentiostat (Wenking model 70 TSI). The measurements were performed in a three electrode cell provided with a copper cathode, a platinum anode and a saturated calomel electrode (SCE). The latter was connected to the cell via a luggin capillary filled with solution under test to minimize contamination.

### 3. Results and discussion

#### 3.1. Cathodic polarization curves

Potentiodynamic current density–cathodic potential curves for both the metals and the alloys were determined under different experimental conditions. The potentials were swept from the zero current values (the rest potential) up to -2000 mV vs SCE at a scan rate of 1 mV s<sup>-1</sup>. The results are shown in Figs 1–5. The individual discharge of each metal is accompanied by large polarization. Tin is predominantly

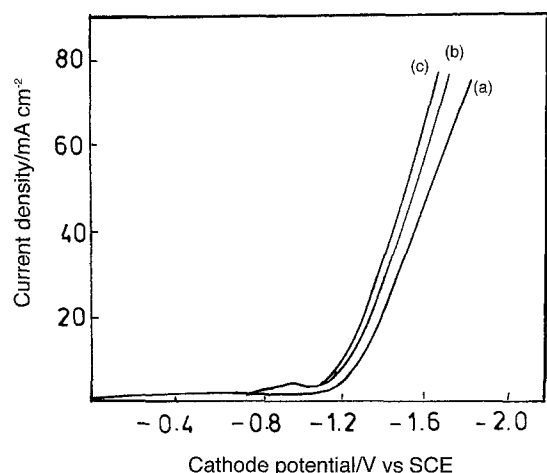


Fig. 2. Cathodic polarization curves for the cobalt deposition at 25°C from solutions containing 20 g dm<sup>-3</sup> K<sub>2</sub>SO<sub>4</sub> and 32 g dm<sup>-3</sup> sodium gluconate and different concentrations of CoSO<sub>4</sub>·7H<sub>2</sub>O: (a) 5, (b) 8, and (c) 18 g dm<sup>-3</sup>.

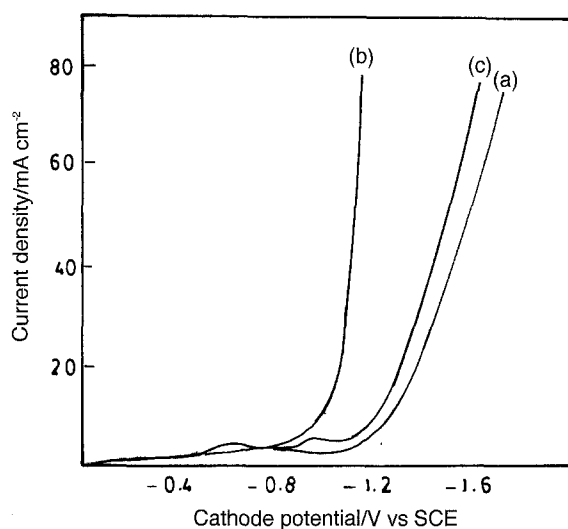


Fig. 3. Cathodic polarization (25°C) curves for the electrodeposition of (a) cobalt from solution containing 8 g dm<sup>-3</sup> CoSO<sub>4</sub>·7H<sub>2</sub>O; (b) tin from solution containing 20 g dm<sup>-3</sup> SnSO<sub>4</sub>; (3) Sn–Co alloy from solution containing 20 g dm<sup>-3</sup> SnSO<sub>4</sub> and 8 g dm<sup>-3</sup> CoSO<sub>4</sub>·7H<sub>2</sub>O. Each solution contained 20 g dm<sup>-3</sup> K<sub>2</sub>SO<sub>4</sub> and 32 g dm<sup>-3</sup> sodium gluconate.

present as the [SnC<sub>6</sub>H<sub>11</sub>O<sub>7</sub>]<sup>+</sup> complex ion in addition to other complex species [7] and cobalt mainly exists as the [CoC<sub>6</sub>H<sub>11</sub>O<sub>7</sub>]<sup>+</sup> complex ion [8]. In Fig. 1, it is clearly seen that tin reduction is strongly inhibited due to the formation of Sn<sup>2+</sup> gluconate complex species. The deposition potential shifts from -800 mV (Fig. 3) to -1600 mV (Fig. 1) as a result of increased stability of the complex species. This negative shift in the tin deposition potential is associated with progressive evolution of hydrogen gas. Thus, a decrease in cathodic current efficiency of tin deposition is expected in dilute solutions. On the other hand, data of Fig. 2 show that cobalt is deposited at about -1200 mV and this deposition potential is hardly affected by change in Co<sup>2+</sup> concentration.

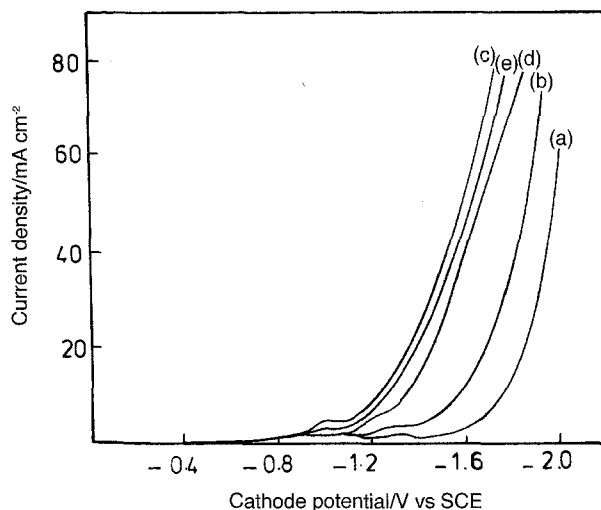


Fig. 4. Cathodic polarization (25°C) curves for the electrodeposition of (a) tin from solution containing 2 g dm<sup>-3</sup> SnSO<sub>4</sub>; (b) from solution containing 5 g dm<sup>-3</sup> SnSO<sub>4</sub>; (c) cobalt from solution containing 8 g dm<sup>-3</sup> CoSO<sub>4</sub>·7H<sub>2</sub>O; (d) Sn–Co alloy from solution containing 2 g dm<sup>-3</sup> SnSO<sub>4</sub> and 8 g dm<sup>-3</sup> CoSO<sub>4</sub>·7H<sub>2</sub>O. (e) Sn–Co alloy from solutions containing 5 g dm<sup>-3</sup> SnSO<sub>4</sub> and 8 g dm<sup>-3</sup> CoSO<sub>4</sub>·7H<sub>2</sub>O. Each solution contains 30 g dm<sup>-3</sup> K<sub>2</sub>SO<sub>4</sub> and 32 g dm<sup>-3</sup> sodium gluconate.

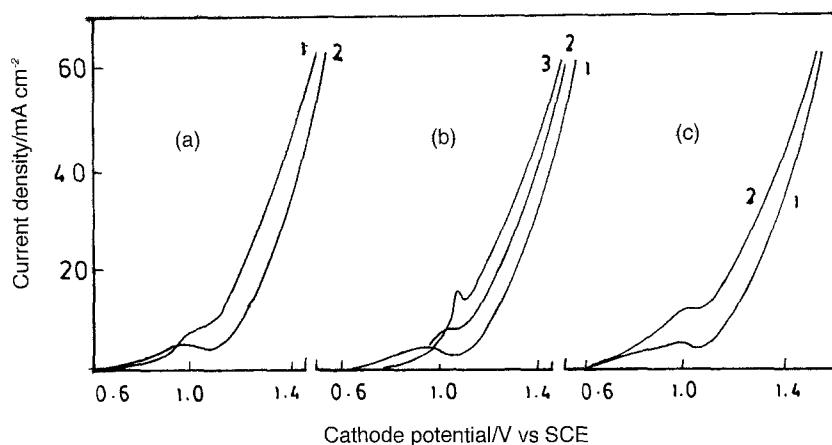


Fig. 5. Cathodic polarization curves for the electrodeposition of Sn-Co alloy from solution containing  $2 \text{ g dm}^{-3} \text{ SnSO}_4$ ,  $8 \text{ g dm}^{-3} \text{ CoSO}_4 \cdot 7\text{H}_2\text{O}$  and  $20 \text{ g dm}^{-3} \text{ K}_2\text{SO}_4$ , curve (a1)  $32 \text{ g dm}^{-3}$  sodium gluconate, (a2)  $64 \text{ g dm}^{-3}$  sodium gluconate, (b1)  $32 \text{ g dm}^{-3}$  sodium gluconate at pH 4.0, (b2)  $32 \text{ g dm}^{-3}$  sodium gluconate at pH 1.7, (c1)  $32 \text{ g dm}^{-3}$  sodium gluconate at  $25^\circ\text{C}$ .

Comparison of the curves of Figs 3 and 4 shows that the relation between the position of the polarization curves of the alloy and those of the parent metals is not uniform and depends greatly upon the concentration of tin ions in the bulk electrolyte. At high tin ion concentrations, the individual polarization curves of tin lay to the left (to the more noble potential) of individual curves of cobalt, indicating that, under such conditions, tin is the more noble component. However, at low concentrations of tin in the bath, its deposition potentials become less cathodic (less negative) than those of cobalt. Under such conditions, cobalt is the more noble component. In all cases it is found that the polarization curves of the alloy lay between those of the parent metals. This is common in many alloy plating systems [10, 11]. This infers that the codeposition enables the less noble metal to deposit at less cathodic (more positive) potentials and causes the more noble metal to deposit at more cathodic potentials than in the individual deposition cases [9].

Figure 5 shows the effect of gluconate ion concentration, pH and temperature on the cathodic polarization of alloy deposition from a bath containing  $5 \text{ g dm}^{-3} \text{ SnSO}_4$ ,  $8 \text{ g dm}^{-3} \text{ CoSO}_4 \cdot 7\text{H}_2\text{O}$ , and  $20 \text{ g dm}^{-3} \text{ K}_2\text{SO}_4$ . In this bath, tin is the less noble component. Increasing the gluconate ion concentration in this bath increases the cathodic polarization mainly as a result of increasing stability of tin gluconate complexes. The deposition potential of the alloy is shifted towards less negative potentials with decrease in pH of the bath as shown in Fig. 5(b). It is possible that this trend is due to a decrease in hydrogen overpotential of the cathode with increasing bath acidity since hydrogen evolution was observed to occur vigorously at low pH values. In addition, in gluconate bath containing tin and cobalt as complexes a variation of pH affects the equilibrium of the complexes unequally. It is possible that the stability of  $\text{Co}^{2+}$  gluconate complex species decreases with increasing bath acidity. This shifts the deposition potential of cobalt in the noble direction and consequently causes easier deposition. However, elevating the bath temperature also decreases the alloy deposition potential, Fig. 5(c). This behaviour may be

attributed to the depolarization effect of temperature on the discharge overpotential of the reducible ions.

### 3.2. Composition of the deposits

Figure 6 shows the influence of tin ion concentration in the bath on the percentage of cobalt in the deposit and on the cathodic current efficiency (CCE) of the alloy deposition at 30 and  $100 \text{ mA cm}^{-2}$ . The broken line AB in the figure indicates the composition reference line which presents the percentage of cobalt in the bath. It is obvious that the cobalt percentage in the deposit decreases markedly with increasing tin content in the bath. At low tin ion concentrations ( $< 8 \text{ g dm}^{-3} \text{ SnSO}_4$ ), the percentage of cobalt in the deposit is above the composition reference line AB, this indicates the preferential deposition of cobalt (the more noble component) suggesting normal codeposition. On the other hand, when the concentration of tin in the electrolyte is raised ( $> 8 \text{ g dm}^{-3} \text{ SnSO}_4$ ),

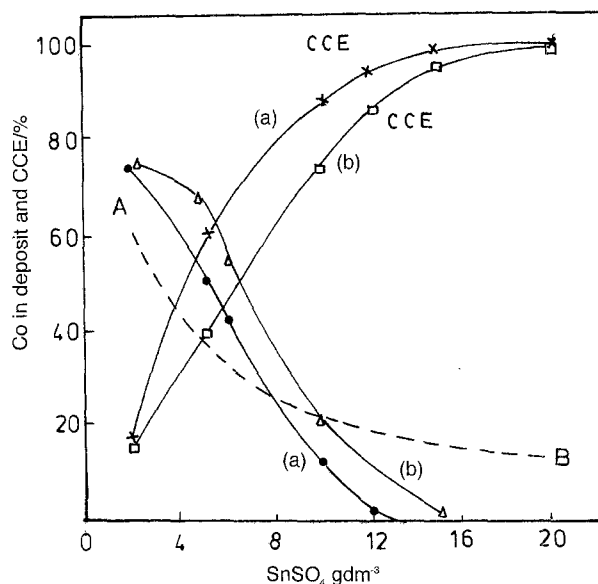


Fig. 6. The effect of the  $\text{SnSO}_4$  concentration on CCE and the composition of Sn-Co alloys from bath containing  $8 \text{ g dm}^{-3} \text{ CoSO}_4 \cdot 7\text{H}_2\text{O}$ ,  $20 \text{ g dm}^{-3} \text{ K}_2\text{SO}_4$ ,  $32 \text{ g dm}^{-3}$  sodium gluconate at  $25^\circ\text{C}$ . Curves: (a) 30 and (b)  $100 \text{ mA cm}^{-2}$ . The reference line AB represents the percentage of cobalt in the bath.

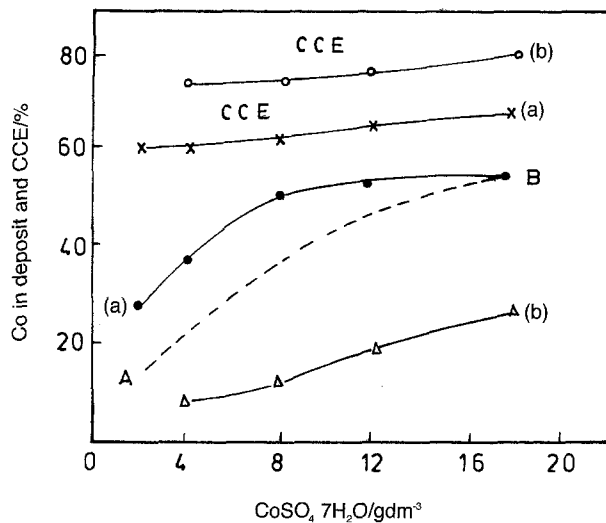


Fig. 7. The effect of the  $\text{CoSO}_4$  concentration on CCE and the composition of Sn-Co alloys at  $25^\circ\text{C}$ , c.d.  $30\text{ mA cm}^{-2}$  and pH 3.9 from baths containing  $20\text{ g dm}^{-3}$   $\text{K}_2\text{SO}_4$ ,  $32\text{ g dm}^{-3}$  sodium gluconate. Curves: (a)  $5$  and (b)  $8\text{ g dm}^{-3}$   $\text{SnSO}_4$ . The reference line AB represents the percentage of cobalt in the bath.

tin becomes the more noble component and so deposits preferentially. This indicates normal codeposition and explains the decrease in the percent of cobalt in the as-deposited alloys. However, with still further increase in the concentration of tin in the bath ( $<14\text{ g dm}^{-3}$   $\text{SnSO}_4$  at  $100\text{ mA cm}^{-2}$  and  $<16\text{ g dm}^{-3}$   $\text{SnSO}_4$  at  $30\text{ mA cm}^{-2}$ ) the deposition of cobalt ceases entirely and the deposits consist only of tin and the CCE tends to reach 100%. This is because the potentials under these conditions are not sufficiently negative to allow the reduction of both  $\text{Co}^{2+}$  and  $\text{H}^+$  ions. These results agree well with the variation of the cathodic polarization of the alloy deposition with the concentration of tin in the bath. It is worth noting that, at a given bath composition, an increase in current density decreases the CCE of the alloy deposition as a result of increasing the cathodic

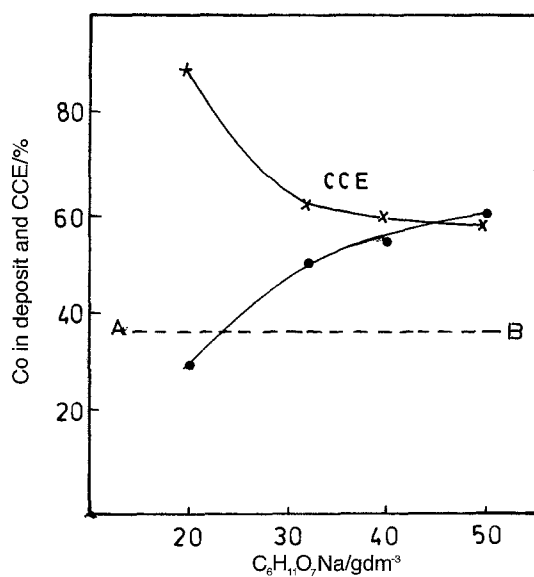


Fig. 8. The effect of the sodium gluconate concentration on CCE and the composition of Sn-Co alloys at  $25^\circ\text{C}$ , c.d.  $30\text{ mA cm}^{-2}$  and pH 3.9 from bath containing  $5\text{ g dm}^{-3}$   $\text{SnSO}_4$ ,  $8\text{ g dm}^{-3}$   $\text{CoSO}_4\cdot 7\text{H}_2\text{O}$  and  $20\text{ g dm}^{-3}$   $\text{K}_2\text{SO}_4$ .

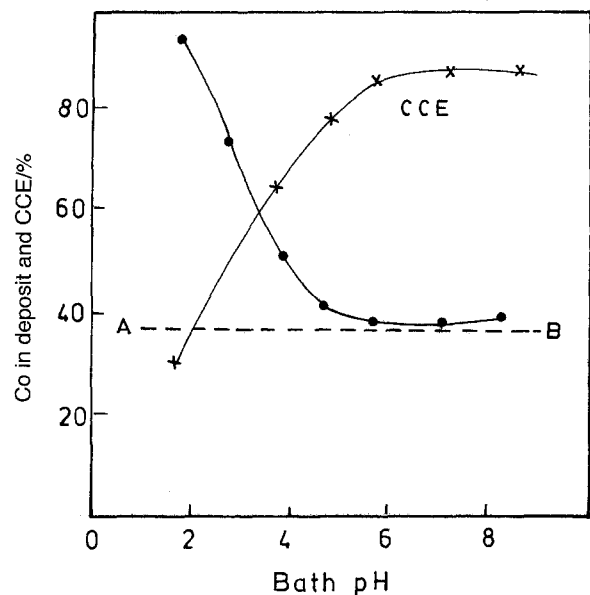


Fig. 9. The effect of bath pH on CCE and the composition of Sn-Co alloys from bath containing  $5\text{ g dm}^{-3}$   $\text{SnSO}_4$ ,  $8\text{ g dm}^{-3}$   $\text{CoSO}_4\cdot 7\text{H}_2\text{O}$ ,  $20\text{ g dm}^{-3}$   $\text{K}_2\text{SO}_4$ ,  $32\text{ g dm}^{-3}$  sodium gluconate at  $25^\circ\text{C}$ , and c.d.  $30\text{ mA cm}^{-2}$ .

polarization which assists the evolution of hydrogen. The cobalt content in the deposit increases slightly with increasing current density irrespective of whether cobalt is the more or less noble metal. This indicates that Sn-Co alloy deposition from these baths can be classified as an irregular plating system. Irregular codeposition is most likely to occur with solutions of complex ions, particularly with systems in which the static potentials of the parent metals are markedly affected by the concentration of the complexing agent [9].

Figure 7 illustrates the relation between the percentage of cobalt in the deposit and its concentration in the bath. The figure reveals that the cobalt content in the deposit increases with increasing bath cobalt, irrespective of whether cobalt is the more noble or not. This result can be attributed to the fact that an increase in the bath cobalt content tends to oppose the depletion of cobalt ions in the cathodic diffusion layer.

Inspection of Fig. 8 reveals that an increase in the gluconate ion concentration causes a decrease in the CCE of alloy deposition and an increase in percent cobalt content in the deposit. This is due to an increase in stability of  $\text{Sn}^{2+}$  complex species and consequent inhibition of the reduction of tin at the expense of the reduction of both cobalt and hydrogen. However, increasing the pH from 1.7 to 8.7 improves the CCE of the alloy deposition as shown in Fig. 9. At low pH, the blocking of the electrode surface by hydrogenated adsorbates may inhibit the discharge of tin and cobalt. Nevertheless, the cobalt content in the deposit initially decreases sharply up to about pH 5 and then becomes almost constant as the percent of cobalt in the bath increases. Similar results have been reported previously [1]. The initial decrease in cobalt content in the deposit is caused by gradual

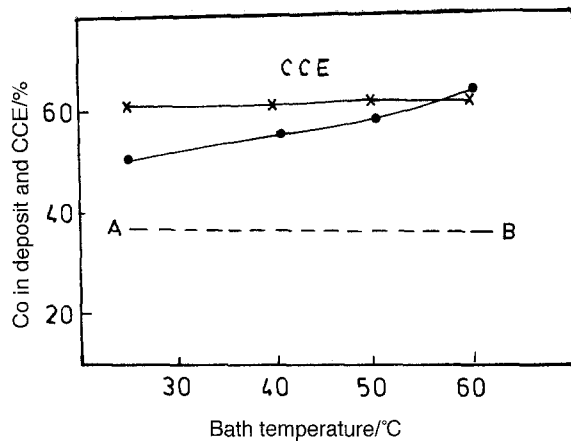


Fig. 10. The effect of bath temperature on CCE and the composition Sn-Co alloys from baths containing  $5 \text{ g dm}^{-3}$   $\text{SnSO}_4$ ,  $8 \text{ g dm}^{-3}$   $\text{CoSO}_4 \cdot 7\text{H}_2\text{O}$ ,  $20 \text{ g dm}^{-3}$   $\text{K}_2\text{SO}_4$  and  $32 \text{ g dm}^{-3}$  sodium gluconate at pH 3.9 and c.d.  $30 \text{ mA cm}^{-2}$ .

decomposition of  $\text{Co}^{2+}$  complex species with increasing the bath pH. This assists the discharge of cobalt. The fact that the alloy composition at pH > 5 becomes almost identical to the line AB indicates that both metal gluconate complexes have nearly the same values of diffusion coefficient and diffusion layer thickness [9].

Figure 10 shows that increase of bath temperature from 25 to  $60^\circ\text{C}$  increases the cobalt content in the deposit but has no significant effect on the CCE of the alloy deposition. An increase in temperature enhances the concentration of metal ions in the cathode diffusion layer, because the rates of diffusion and of convection increase with temperature. An increase in metal concentration at the solution-cathode interface favours increased deposition of cobalt which is already depositing preferentially under such conditions.

### 3.3. Structure of the deposits

The alloy deposits were generally adherent, bright and similar to chromium in appearance. The brightness of the deposit was enhanced with increasing bath temperature but decreased with increasing current density. The surface morphology of the as-plated tin-cobalt alloys deposited under different conditions were examined by scanning electron microscopy. Some of the SEM micrographs are shown in Fig. 11. These showed that the deposit obtained at low current density ( $30 \text{ mA cm}^{-2}$ ) is compact. The deposit consists of regularly oriented nodular fine grains Fig. 11(a). Increasing the bath temperature increases the grain size, Fig 11. (b). This may be due to the decrease in cathodic polarization. The decrease in polarization may retard the nucleation rate and favour the formation of coarse grains [6]. It is worth observing that at high current density ( $100 \text{ mA cm}^{-2}$ ) the deposition is not uniform and is composed of irregular grains which are grouped together in a random orientation and which include some pores. These features appear to be related to evolved and/or adsorbed hydrogen on the cathode surface Fig. 11(c).

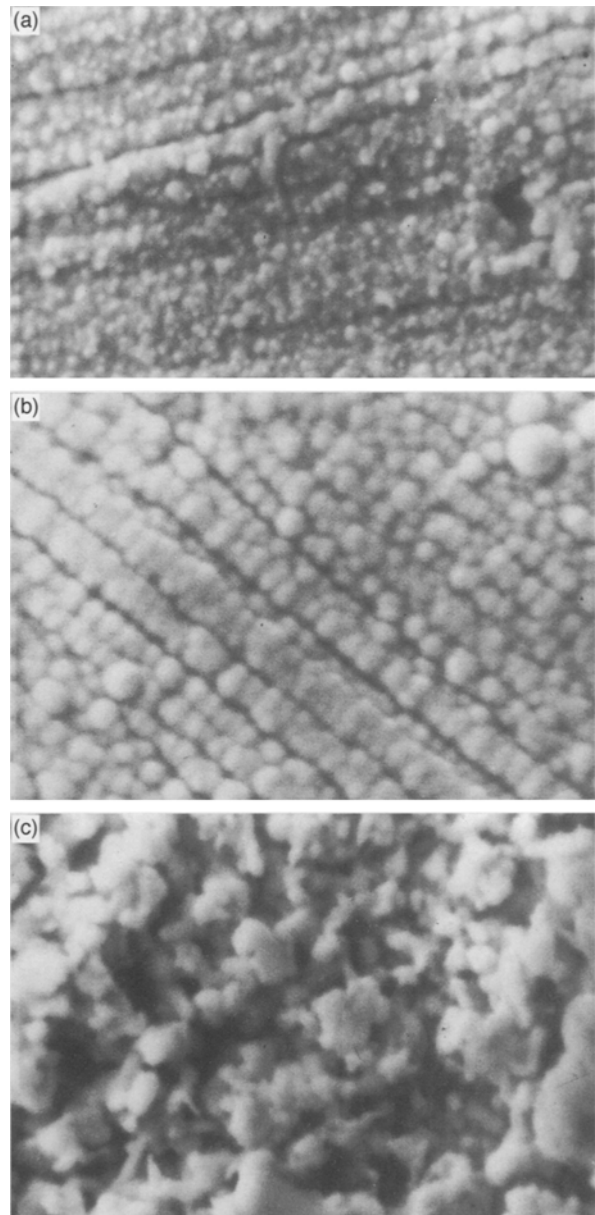


Fig. 11. Scanning electron micrographs of Sn-Co alloy from a bath containing  $5 \text{ g dm}^{-3}$   $\text{SnSO}_4$ ,  $8 \text{ g dm}^{-3}$   $\text{CoSO}_4 \cdot 7\text{H}_2\text{O}$ ,  $20 \text{ g dm}^{-3}$   $\text{K}_2\text{SO}_4$  and  $32 \text{ g dm}^{-3}$  sodium gluconate at pH 3.9, duration of electrolysis 20 min, at (a)  $30 \text{ mA cm}^{-2}$ ,  $25^\circ\text{C}$  (b)  $30 \text{ mA cm}^{-2}$ ,  $50^\circ\text{C}$ , (c)  $100 \text{ mA cm}^{-2}$ ,  $25^\circ\text{C}$ .

X-ray diffraction studies of the deposits (in as-deposited conditions) revealed that the phase structure of the deposits is controlled by their composition. Data of Table 1 show that the cobalt rich alloy (74% of cobalt) is composed mainly of a hexagonal close packed  $\text{Co}_3\text{Sn}_2$  phase in addition to a minor quantity of the hexagonal close packed  $\alpha$ -Co lattice structure. On the other hand, the tin rich alloy (88% of tin) consists mainly of a tetragonal  $\text{CoSn}_2$  phase with minor quantity of tetragonal crystals with the  $\beta$ -Sn form.

### 4. Conclusion

Adherent, smooth and very bright deposits of Sn-Co alloys can be electroplated onto copper substrates from gluconate baths. The effect of some plating

Table 1. X-ray diffraction for Sn-Co alloys electrodeposited from solutions containing: sample (I)  $2 \text{ g dm}^{-3} \text{ SnSO}_4$  and  $8 \text{ g dm}^{-3} \text{ SnSO}_4$   $8 \text{ g dm}^{-3} \text{ CoSO}_4 \cdot 7\text{H}_2\text{O}$ ; sample (II)  $10 \text{ g dm}^{-3} \text{ SnSO}_4$  and  $8 \text{ g dm}^{-3} \text{ CoSO}_4 \cdot 7\text{H}_2\text{O}$ .\*

Sample	Alloy composition/%		d/nm	i/j <sup>0</sup>	Average lattice parameters/nm		Phase
	Sn	Co			a	c	
I	26	74	0.2045	14.6	0.4107	0.5180	hexagonal Sn <sub>2</sub> Co <sub>3</sub>
			0.2759	26.7			hexagonal α (Co)
			0.2172	52.0	0.2508	0.4053	hexagonal α (Co)
			0.1913	34.0			
II	88	12	0.2071	14.0	0.6361	5.454	tetragonal CoSn <sub>2</sub>
			0.2527	100.0			tetragonal β (Sn)
			0.2918	100.0	0.5841	0.3132	tetragonal β (Sn)
			0.2024	67.0			

\* Each solution contained  $20 \text{ g dm}^{-3} \text{ K}_2\text{SO}_4$  and  $32 \text{ g dm}^{-3}$  sodium gluconate at c.d. =  $30 \text{ mA cm}^{-2}$ ,  $t = 25^\circ\text{C}$ , duration 20 min.

variables on the cathodic current efficiency, composition and structure of the alloy deposits were studied. An explanation has been offered for the various trends observed in the light of cathodic polarization. The optimum conditions are:  $5 \text{ g dm}^{-3} \text{ SnSO}_4$ ,  $8 \text{ g dm}^{-3} \text{ CoSO}_4 \cdot 7\text{H}_2\text{O}$ ,  $20 \text{ g dm}^{-3} \text{ K}_2\text{SO}_4$  and  $32 \text{ g dm}^{-3}$  sodium gluconate, c.d.  $30 \text{ mA cm}^{-2}$ , pH 5.5 and  $40^\circ\text{C}$ .

## References

- [1] J. D. C. Hemsley and M. E. Roper, *Trans. Instit. Metal. Finish.* **57** (1979) 77.
- [2] H. C. Jennison and J. C. Bradley, *US Patent* 2 336 615 (1943).
- [3] J. Ireland and N. Parkinson, *US Patent* 2 658 866 (1953).
- [4] V. Sree and T. L. Rama Char., *J. Electrochem. Soc. (India)* **9** (1960) 13.
- [5] M. Clark, R. C. Elbourne and C. A. Mackay, *Trans. Instit. Metal. Finish* **50** (1972) 180.
- [6] S. S. Abd El Rehim, A. M. Abd El Halim and M. M. Osman, *J. Chem. Tech. Biotechnol.* **35A** (1985) 415.
- [7] T. M. Maskin, B. Z. Zmbova and D. S. Veseliñovic, *J. Serb. Chem. Soc.* **56** (1991) 337.
- [8] F. J. Ashton and W. F. Pickering, *Aust. J. Serb. Chem.* **23** (1970) 1367.
- [9] A. Brenner, 'Electrodeposition of Alloys,' Vol. 1, Academic Press, New York (1963).
- [10] A. M. Abd El Halim, S. S. Abd El Rehim, S. M. Abd El Wahaab and E. A. Abd El Meguid, *J. Appl. Electrochem.* **17** (1987) 667.
- [11] S. S. Abd El Rehim, A. Awad and A. El Sayed, *ibid* **17** (1987) 156.